International Journal of Advanced Science and Research
ISSN: 2455-4227
Impact Factor: RJIF 5.12
www.allsciencejournal.com
Volume 2; Issue 5; September 2017; Page No. 39-44

Enhanced photoconduction in CdTe QD decorated ZnO NWs

[1] Vandana Taori, [2] Anjali Oudhia, [*3] Neelam Shukla, [4] Poonam Bichpuria
[1] MAT University, Raipur, Chhattisgarh, India
[2, 4] Government Nagarjuna P.G. Science College, Raipur, Chhattisgarh, India
[3] Kalyan P.G. Autonomous College, Bhilai, Chhattisgarh, India

Abstract
CdTe QD decorated ZnO NWs arrays ((CdTe@ZnO)) are controllably synthesized by using simple microwave assisted (MW) and Chemical bath deposition (CBD) wet chemical strategy in this paper. The effect on structural and morphological of CdTe@ZnO was investigated by X-ray diffraction (XRD) and SEM. The CdTe QDs were densly and uniformly coated on ZnO NWs both radially and along the axial direction, and forms an intact interface with the wurtzite ZnO NWs core as observed in the SEM. The as-prepared CdTe@ZnO are found to exhibit significantly enhanced photoconduction as compared to the pristine ZnO NWs arrays, attributed to the decreased band gap and / or depletion of oxygen vacancies and other defects states in them. Furthermore, the effect of CdTe QDs loading on the absorbance and photoconductive performances of CdTe@ZnO are also investigated. The absorption and photoconduction of the CdTe shell above its band gap (1.5 eV) respectively, are demonstrated by absorption and photoconductivity measurements.

Keywords: FTO, nanowires, photoconductivity, ZnO, CdTe decorated ZnO NWs

1. Introduction
One-dimensional semiconductor nanostructures are considered as the most sensitive and fast responsive materials for photon conduction due to their large surface-to-volume ratio and direct pathway for charge transport [1-3]. A variety of semiconductor NWs and nanoribbons of group II-VI compounds e.g. ZnO, ZnS, CdS, CdSe, CdTe have been developed for optoelectronic devices, as the active materials covering the whole spectrum from for UV to visible and infrared light [4-6]. However, pure semiconductor NWs cannot absorb wavelengths below their band gap, which limits their wide spectral sensitivity in standard devices, such as for visible or ultraviolet (UV) light imaging, memory storage or switches. QDs open up new possibilities for the multiple charge carrier generation with a single photon [7-8]. Multiple carrier generation in nanocrystals has shown that two or more excitons can be generated with a single photon of energy greater than the band gap. Semiconductor quantum dots (QDs) such as CdS, CdSe, PbS, PbSe, InP and InAs have recently been extensively used as light harvesters in the application of QD-sensitized solar cells (QDSSCs).Unique size and shape dependent absorption properties of quantum dots or nanocrystals are hosted on a transparent electrode, which consists of a one-dimensional (1D) ZnO NWs on a conducting substrate. In such a configuration, an appropriate band alignment between the QDs and the ZnO NWs allows efficient charge carrier injection, and 1D nanostructures provide an ideal channel for effective carrier transport. CdTe has a high optical absorption coefficient and narrow band gap of 1.5 eV matching the preferred range of the solar radiation spectrum. It allowing effective injection of photogenerated electrons from CdTe into ZnO. Consequently, CdTe@ZnO forms a nanocable array on a transparent conductive substrate would hold great potential in a number of photoelectrical and photoconducing applications. Several methods may be used to deposit a semiconductor material shell on an FTO substrate i.e. Electrochemical Deposition, Microemulsion method, Chemical bath deposition (CBD) methods [9, 10]. CBD is preferable for ZnO NWs preparation as it is relatively simple, scalable, cost effective and can produce dense NWs. In the present work, CdTe QDs were prepared by (microwave) MW assisted method [11, 12]. Good absorption, photoconduction properties between the CdTe shell and the ZnO core are demonstrated by absorption and photoconductivity (PC) measurements, respectively. In present work, a simple, low-cost, catalyst free and direct mass-scale production method is applied for the preparation of high-purity ZnO/CdTe QDs core-shell NWs samples have been studied for their optical and photoconduction properties.

2. Experimental procedure
2.1. Preparation of ZnO NWs Arrays
Firstly the microscopic glass substrates were cleaned by immersing them in a mixture of aqueous hydrogen peroxide (H_2O_2) and concentrated hydrochloric (HCl) acid (1:3) for 20 h, washed with deionized water under ultrasonication and then dried in air. All chemicals were analytical grade (Merck), and were used without further purification. Double distilled water (DDW) was used in experiment. The two-step method was adopted to fabricate ZnO/CdTe NWs arrays. The FTO glass substrates were ultrasonically rinsed for 0.5 h in acetone, isopropyl alcohol, and ethanol solution, respectively. The ZnO seed layers were first deposited on FTO substrates by dip-coating method. After heat treatment at 400 °C for 1 h, the

FTO coated with seed layers was immersed in an aqueous solution containing 0.05 M zinc nitrate (Zn(NO3)2) and 0.05 M hexamethylenetetramine (HMTA) and was kept in a water bath for 5h at 90 °C, for synthesis of ZnO NWs by CBD method. Fabricated ZnO NWs arrays were washed with deionized water and were dried and annealed at 350°C in a muffle furnace. The furnace was naturally cooled down to room temperature to obtain ZnO NWs arrays synthesized on the FTO.

2.2 Synthesis of ZnO/CdTe core-shell NW arrays

The synthesis of nano CdTe and their subsequent coating on ZnO NWs was done as follows: $CdCl_2$ $5H_2O$ was diluted with 40 ml of Toluene. During a constant stirring GSH, Sodium citrate, K_2TeO_3 sol and $NaBH_4$ were added into Cadmium sol. 1M NaOH was then used to adjust the pH 10 under vigorous stirring. The mixture was kept in a MW oven for 1 min at 300W. The mixture was cooled down to ~ 50ºC. The as prepared CdTe solution was concentrated to ¼ th of the original volume, was precipitated using 2-propanol and was finally collected via centrifugation. CdTe dispersion was prepared by re-dissolving this colloid precipitate in 3ml DD water and was kept for the CdTe coating on ZnO NWs arrays. It may be noted that to study of effect of growth of CdTe coating on ZnO NWs arrays, we tried various molar concentration of CdTe and various time for deposition of CdTe layer. The optimized molar concentration and deposition time for maximum photocurrent and optical absorption was used for further study. A weight ratio of 5% of CdTe was added to 10mL of water and ultrasonicated it for 30 min. The FTO substrate deposited with ZnO NWs was dipped into this solution and was kept on a magnetic stirrer at 60°C at 600 rpm. After the evaporation of water, the substrates were annealed at 350 ◦C in a muffle furnace under ambient condition. Finally we obtained the sample of CdTe@ZnO. The final products were left to cool at room temperature. The pieces were taken out and dried before the subsequent characterization.

3. Result &discussion

3.1 SEM Studies: The morphology of the as prepared CdTe@ZnO were observed in SEM. Fig. 1(a) and fig.1(b) shows the typical SEM images of pristine ZnO NWs sample and CdTe@ZnO synthesized by wet chemical methods. It can be seen clearly that the orderly hexagonal and densely populated ZnO NWs arrays are grown onto the FTO glass substrates. In fig.1 (a) the diameter and length of ZnO are 110–200 nm and~2.5μm respectively. After CdTe coating the as-prepared ZnO NWs film changed from white to black, implying the formation of CdTe on the ZnO NWs surface.Whereas spherical CdTe particles can be observed around the ZnO NWs observed in fig. 1(b). The CdTe@ZnO are observed to be much thinner in fig.1(b), which may be due to etching and dissolution of ZnO NWs during the coating of CdTe QDs [13].

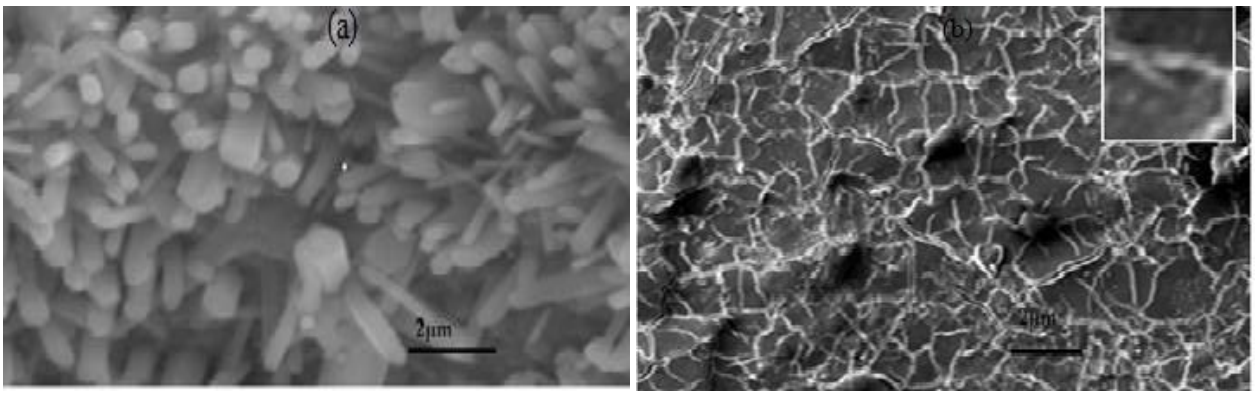

Fig 1: SEM images of (a) ZnO NWs grown on FTO (b) CdTe@ZnO grown on FTO

3.2 XRD: The X-ray diffraction (XRD) spectra taken from pure ZnO NWs arrays and as deposited CdTe@ZnO are shown in fig.2 (a) and 2(b) respectively. For pure ZnO NWs arrays, eight diffraction peaks can be respectively indexed to the (100), (002), (101), (102), (110), (103), (201) and (202) planes of wurtzite phase ZnO (JCPDS file No.74-534) [14]. The predominant (101) peaks suggest that the ZnO NWs grew with their *c*-axis orientation normal to the FTO surface. After deposition of CdTe two new peaks are observed in addition to the diffraction peaks from the hexagonal ZnO NWs in fig. 2(b). These broad peaks are centered at 23.96° and 39.40° which can be indexed respectively to the (111) and (220) planes of the zinc-blende (ZB) CdTe (JCPDS file No. 65-880). The emergence of new independent peaks of CdTe suggests that CdTe QDs are not forming a single phase with ZnO, and are just decorated on the NWs. The XRD results are supported by the SEM micrographs too, where CdTe decorated ZnO NWs can be observed in abundance. The average grain size (D) of the ZnO NWs arrays and as deposited CdTe@ZnO was calculated with the help of Scherrer formula in Eq. (1) using the diffraction intensity of (101) peak [15, 16].

$$D = k\lambda/(\beta \cos \theta) \quad (1)$$

where λ is the X-ray wavelength, β is the full width at half maximum (FWHM) of the ZnO (101) line and θ is the diffraction angle. The broadening of the diffraction peaks is an indication that the synthesized materials are in nanometer regime [17-19]. The grain size was obtained 23nm and 11 nm respectively in the range of the ZnO NWs arrays and as deposited CdTe@ZnO.

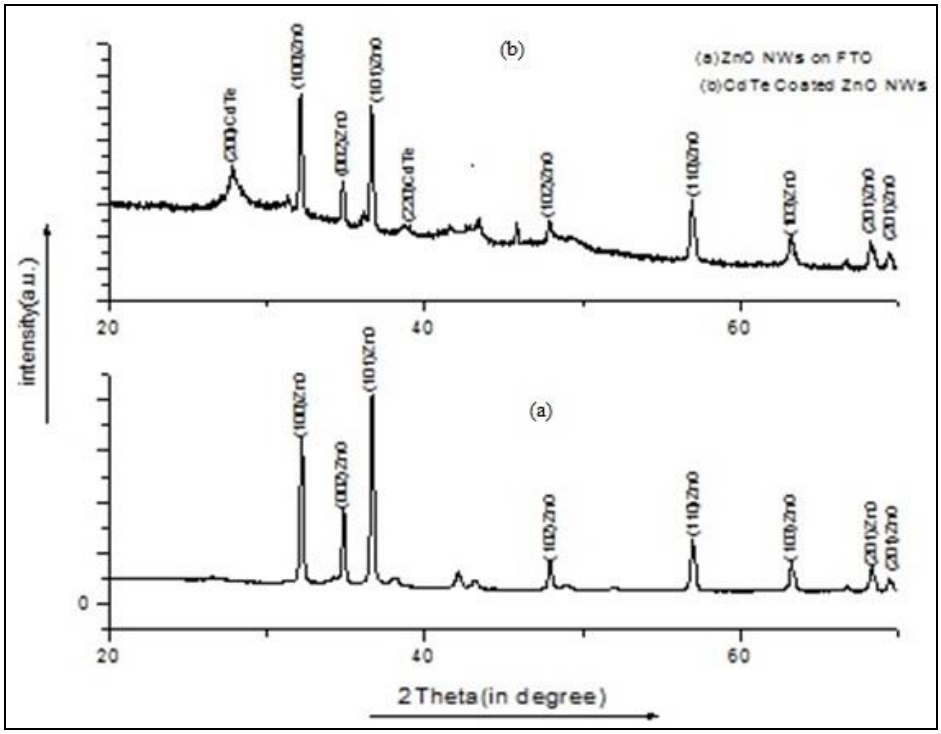

Fig 2: XRD patterns of (a) ZnO NWs grown on FTO (b) CdTe QDs coated ZnO NWs grown on FTO

3.3: Optical absorption study: UV visible absorption spectra of ZnO NWs in fig.3(a) exhibits a clear sharp absorbance peak in the UV region at 368 nm whereas in case of CdTe@ZnO in fig 3(b) exhibits remarkably red shifted absorbance edge, showing an onset of absorption at 670 nm covering the whole visible region[20,21]. RED shift in the absorption edge after decoration with CdTe QDs towards higher wavelength is very favourable as it extends the range of absorption spectra from UV to visible thereby making it a suitable window material for solar cell. An optical band gap of 1.85 eV estimated for the CdTe@ZnO layer from the absorption spectra given in table I, is much less than the band gap of the as prepared ZnO NWs.

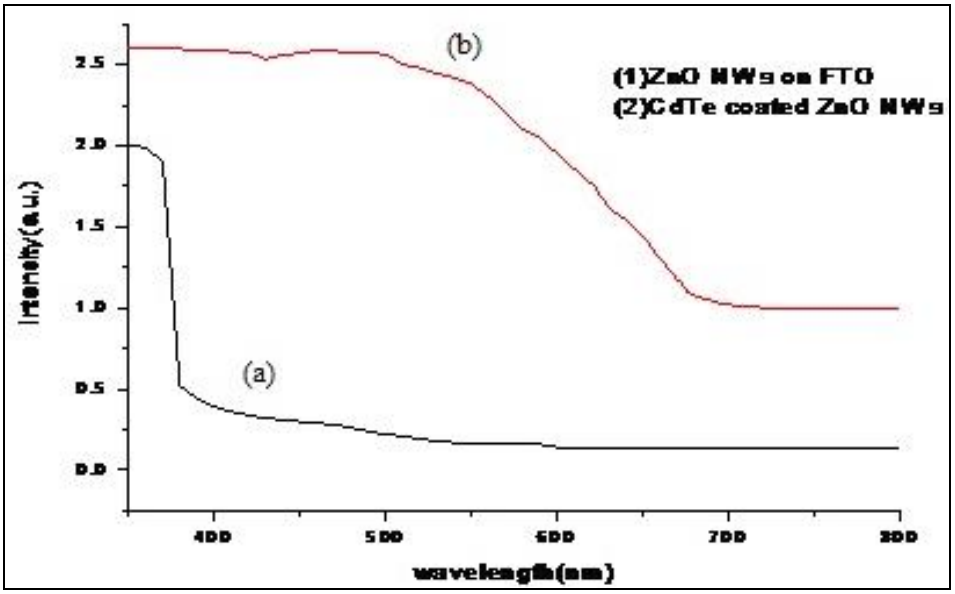

Fig 3: Absorption spectra of (a) ZnO NWs grown on FTO (b) CdTe @ ZnO NWs grown on FTO

Table 1: Band gap of as prepared ZnO NWs and CdTe@ZnO NWs from absorption spectra

Sample	λ (nm)	Band gap Energy (eV)
a. ZnO NWs	368	3.378
b. CdTe@ ZnO NWs	670	1.850

3.4. Photoconductivity study

The PC was measured in an assembled setup using regulated power supply as a voltage source and a commercial 100 W incandescent bulb as a photo-excitation source. The response behavior of the thin film was characterized by measuring

photocurrent as a function of time and voltage. Generally, ZnO NWs are n-type semiconductor due to oxygen vacancies and other native defects such as interstitial Zn ions which act as donors in ZnO lattice. It is well known that the rise and decay curves of photocurrent are governed by the trapping states and recombination centers lying inside the material. Therefore these curves can be used to understand the nature and distribution of traps and recombination centers. The response time is an important property of photoconductive materials. If trapping centers are in abundance, the response time is slow. Trapping also increases the decay time, as the carriers are slowly released after removal of the excitation source. Extensive study of photoconducting properties has been made in nanoparticles, thin films, nanorods, NWs and mixed lattice for different parameters.

3.4.1. Time-resolved growth and decay of photocurrent: Fig. 4 (a) shows growth and decay of photocurrent spectra of ZnO NWs and fig 4(b) shows CdTe@ ZnO NWs samples under illumination of light. In ZnO NWs sample the photocurrent reaches a maximum value of 81.27 mA When light in switched on, and then starts decaying during steady illumination [22]. In fig. 4 (b) for CdTe@ZnO sample when light is switched on, the photocurrent reaches a maximum value of 102.98 mA and then starts decaying during steady illumination. Similar results have been reported by A. Bera *et al*. [23]. Slow rise and decay may be attributed to dominance of surface related processes of adsorption and desorption of oxygen molecules [24]. This confirms that the thinner CdTe@ZnO NWs with higher surface to volume ratio enhances photoconduction by modifying the grain boundaries and thereby providing easy pathways for electron conduction.

$$\text{PC Gain} = I_{ph}/I_{dc} \quad (2)$$

I_{ph} is photocurrent and I_{dc} is dark current. The photocurrent on–off ratio as I_{ph}/I_{dc} is critical parameter to determine the photosensitivity of the films, where I_{ph} is the difference between the total current to the current when light is turned on and I_{dc} is the dark current. The maximum photoresponse was observed for CdTe QDs coated ZnO NWs. PC Gain of ZnO NWs and CdTe@ZnO NWs are obtained as $2X10^2$ and $3.5X1o^3$ respectively.

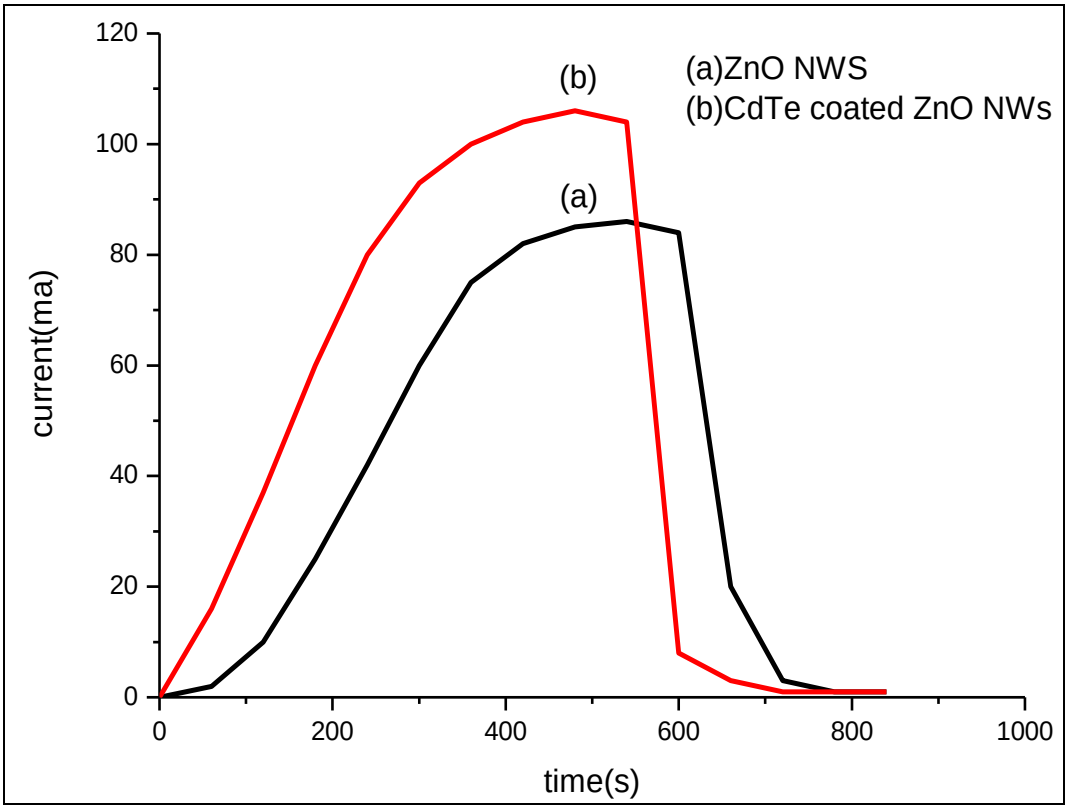

Fig 4: Rise and decay curve of (a) ZnO NWs grown on FTO (b) CdTe @ ZnO NWs grown on FTO

3.4.2 Study of voltage dependence of photocurrent: Fig. 5(a) shows the variation of photocurrent (I_{pc}) with voltage for ZnO NWs and fig. 5(b) for CdTe@ZnO NWs grown on FTO sample. In fig 5(a) ZnO NWs sample show linear variation of current with applied voltage but in fig. 5(b) for CdTe @ ZnO NWs a sudden exponential increase in PC is observed after initial linear region, with applied voltage [25]. At higher voltage the current flow through the samples is limited by space charge. However, at high voltages, the current is no longer determined by the carrier densities that were present without any field. Due to large surface to volume ratio of ZnO NWs adsorption desorption of O2 molecules on surface play important role in current enhancement. The photocurrent increases which may be due to removal of the adsorbed oxygen molecules from the surface thereby releasing trapped carriers for conduction. After CdTe QDS decoration

enhancement in photocurrent can be attributed to three important factors of the CdTe @ZnO NWs based solar cell: strong light absorption in a wider wavelength range, higher CdTe QDs coated on ZnO NWs surface, and direct contact between CdTe and ZnO without any interlinking material[26].

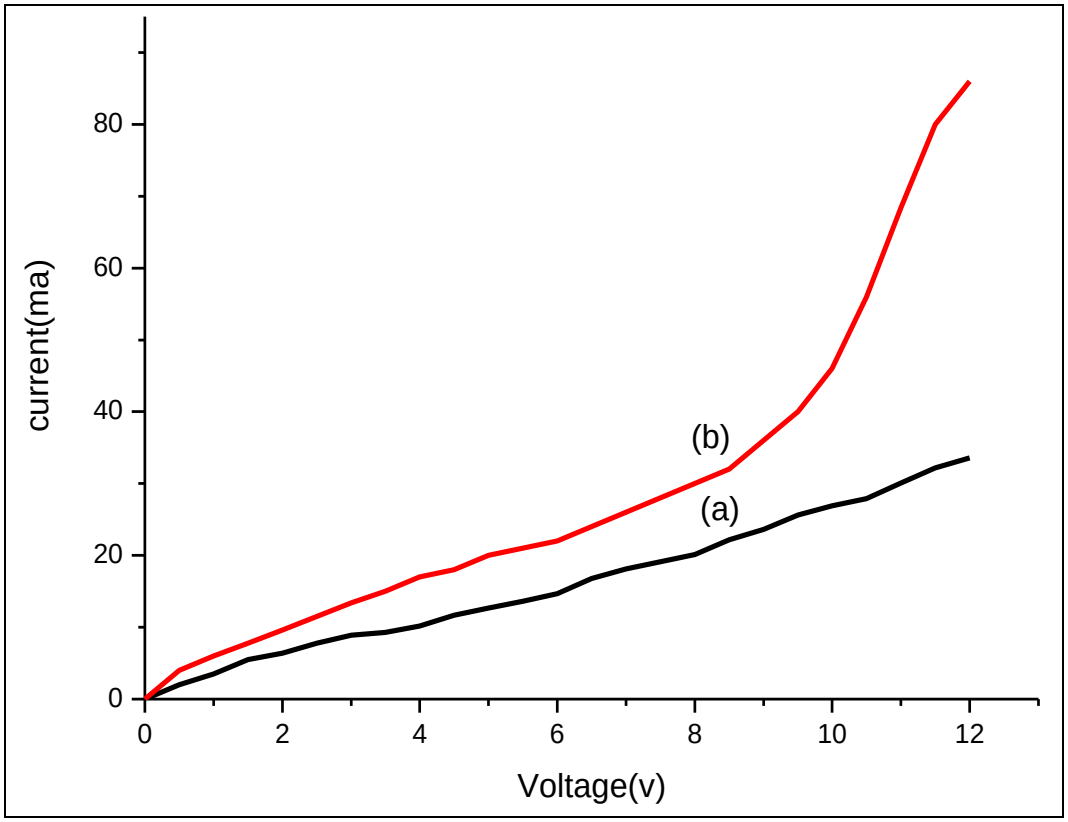

Fig 5: Voltage dependence of photocurrent (a) ZnO NWs grown on FTO (b) CdTe @ ZnO NWs grown on FTO

4. Concussion

In summary, ZnO NW and CdTe@ZnO QDs NWs were successfully synthesized via a simple two-step wet chemical synthesis process. We have demonstrated the photoconductive performances of CdTe@ZnO exhibiting significant enhancement in the photocurrent as a function of time and voltage as compared to pristine ZnO NWs arrays. The favorable absorption properties of CdTe@ZnO configuration contributes to a better performance in photonic applications. Moreover, this controllable wet chemical process provides a facile way for the rational construction of ZnO-based and other metal oxide-based nanostructures in optoelectronic and photovoltaic applications.

5. Acknowledgements

The authors are grateful to the lab facilities made available at the Government VYT PG Autonomous College Durg, Kalyan PG autonomous college, Bhilai and Pt RSS University, Raipur (CG).

6. References

1. Lieber CM, Wang ZL. MRS Bull. 2007; (32):99-104.
2. Liu S, Ye JF, Cao Y, Shen Q, Liu ZF, Qi LM *et al*. Small. 2009; (5):2371-237.
3. Lao CS, Park MC, Kuang Q, Deng YL, Sood AK, Polla DL *et al*. J. Am. Chem. Soc. 2007; 129:12096-12097.
4. Soci C, Zhang A, Xiang B, Dayeh SA, Aplin DPR, Park JD *et al*. Nano Lett. 2007; (7):1003-1009.
5. Fang XS, Bando Y, Liao MY, Gautam UK, Zhi CY, Dierre B *et al*. Adv. Mater. 2009; (21):2034-203.
6. Wei TY, Huang CT, Hansen BJ, Lin YF, Chen LJ *et al*. Appl. Phys. Lett. 2010; (96):013508.
7. Schaller RD, Agranovich VM, Klimov VI. Nat. Phys. 2005; (1):189-194.
8. Schaller RD, Klimov VI. Phys. Rev. Lett. 2004; (92):186601.
9. Gupta S, Oudhia A, Choudhary A. IJARSE, 2015; 4(1).
10. Bichpuria P, Oudhia A, Kulkarni P. Journal of biotechnology and biochemistry. 2017; 3(3):60-64.
11. Reed CE, Scott CG. Br. J. Appl. Phys. 1968; (1):1125.
12. Bichpuria P, Oudhia IJLA. 2016; (1):101-103.
13. Mishra SK, Srivastava RK, Prakash SG, Yadav RS, Pandey AC, Electron. Mater. Letts. 2011; (70):31.
14. Kripal R, Gupta AK, Mishra SK, Srivastava RK, Pandey AC, Prakash SG. Spectrochim. Acta, Part A, 2010; (76)523.
15. Maurya A, Chauhan P, Mishra SK, Srivastava RK, J. Alloys Compd. 2011; 509:8433.
16. Ahn SE, Lee HS, Kim H, Kim S *et al*. Appl. Phys. Lett. 2004; 84:5022.
17. Ahn SE, Ji HJ, Kim K, Kim GT, Bae CH, Park SM *et al*. Appl.Phys. Lett. 2007; (90):153106.
18. Bera A, Basak D, Appl. Phys. Lett. 2008; (93):053102.
19. Srivastava RK, Prakash SG. Natl. Acad. Sci. Lett. 2007;

(30):11.
20. Peng L, Zhai J-Li, Wang D-J, Wang P, Zhang Y *et al*. Chem. Phys. Lett. 2008; 456:231.
21. Panigrahi S, Bera A, Basak D. Appl. Mater. Inter. 2009; (1):2408.
22. Oudhia A, Shukla N, Bose P, Lalwani R, Choudhary A. Nano-Structures & Nano-Objects. 2016; (7):0-5.
23. Bera A, Basak D, Appl. Phys. Lett. 2009; (94):163119.
24. Devi S, Prakash SG, Pramana J. Phys. 1992; (39):145.
25. Devi S, Prakash SG, Pramana J. Phys. 1994; (43):245.
26. Leschkies KS, Divakar R, Basu J, Enache-Pommer E, Boercker JE, Carter CB *et al*. Nano Lett. 2007; (7):1793.